Brugia *et al.*
The Journal of Headache and Pain (2025) 26:85
https://doi.org/10.1186/s10194-025-02030-2

The Journal of Headache and Pain

RESEARCH

Open Access

Inhibition of endocannabinoid hydrolases MAGL, FAAH and ABHD6 by AKU-005 reduces ex vivo cortical spreading depression

Flavia Brugia[1], Konstantin Ivanov[2], Auni Aroviita[2], Raisa Giniatullina[1], Marko Lehtonen[3], Tarja Malm[1], Juha Savinainen[2], Rashid Giniatullin[1] and Adriana Della Pietra[1*]

Abstract

Background Migraine is a common neurovascular disorder that remains currently untreated in half of the patients. One third of migraine patients experience aura, which is associated with the development of cortical spreading depolarization (CSD), a wave of depolarization involving neurons and glial cells. Cannabinoids have proven to be a promising class of compounds for the treatment of migraine pain. In this study, we are proposing a new strategy to counteract development of CSD and downstream events via multicomponent enhancement of the endocannabinoid system (ECS) by using a AKU-005, to simultaneously target several key endocannabinoids hydrolases. To this end, we profiled the activity of selective endocannabinoid hydrolases and their inhibition by AKU-005 and analyzed the effect of AKU-005 on the development of CSD in an ex vivo cortical slice model.

Methods The inhibitory profile of AKU-005 was evaluated by a glycerol assay of lysates from HEK293 cells expressing mouse and human MAGL and ABHD6. After ex vivo treatment of cortex slices of Wistar rats and C57 BL/6 J-OlaHsd mice, endocannabinoids were quantified by mass spectrometry (LC–MS/MS), and activity of the hydrolases MAGL, FAAH, and ABHD6 were measured by activity-based protein profiling (ABPP). The effect of AKU-005 on ex vivo CSD wave in cortical slices was studied by live calcium imaging.

Results Ex vivo, AKU-005 inhibited MAGL, FAAH, and ABHD6, increasing 2-arachidonoylglycerol (2-AG) and anandamide (AEA) levels in rat cortex under both basal and CSD conditions. In mice, AKU-005 showed a milder effect, inhibiting MAGL only under CSD conditions and increasing 2-AG levels in both basal and CSD states. In vitro analyses confirmed the ex vivo findings for rats and revealed basal MAGL inhibition in mice cortex. AKU-005, previously reported as a double MAGL/FAAH-inhibitor, also inhibited overexpressed mouse and human ABHD6, a little studied 2-AG-hydrolyzing enzyme in brain. In line with these results, AKU-005 reduced CSD events in cortical slices from both rodent species, with higher efficacy in rats.

Conclusions Given the distinct profile of endocannabinoids hydrolases activities between rats and mice in the brain areas associated with migraine, AKU-005 may target multiple endocannabinoid hydrolases to serve as an efficient treatment option for migraine with aura.

Keywords Headache, Endocannabinoids, Pain, Serine hydrolases, CSD

*Correspondence:
Adriana Della Pietra
adellapietra@uiowa.edu
Full list of author information is available at the end of the article

Background

The peripheral trigeminovascular system plays a crucial role in triggering migraine pain by activating trigeminal nerve terminals and by releasing calcitonin gene-related peptide [1, 2], which causes meningeal vessel dilation [3], mast cell degranulation [4] and inflammation [5], sensitizing both peripheral and central neurons [6], and transmitting nociceptive signals to the CNS, leading to migraine pain perception [7]. In migraine with aura, which affect about 1/3 of migraine patients, the central nervous system could be involved early on by an event known as cortical spreading depolarization (CSD), a wave of strong neuronal depolarization followed by inhibition [8]. From the therapeutical perspective, CSD represents one of the potential targets for reducing the harmful hyperexcitable brain state associated with elevated glutamate release [9, 10]. CSD is considered as a trigger of headache [11, 12] operating via several mechanisms, including the transit of cerebrospinal fluid (CSF) molecular triggers from cortical areas directly to the trigeminal neurons [13].

While the capacity of cannabinoids to reduce migraine headache has been suggested [14–17], their action on CSD has been less studied and is not clear. The ability of cannabinoids to reduce the release of glutamate in synaptic contacts may suggest that the activation of the ECS modulates migraine-related CSD [18]. Previously, one study suggested that neither anandamide (AEA) nor the CB1/2 agonist WIN 55.212–2 affect characteristics of CSD elicited by high potassium application [19]. On the other hand, another study showed that WIN 55.212–2 instead inhibited the amplitude, duration and velocity of CSD propagation, while JWH 133, a CB2 receptor agonist, did not have any modulatory effect [20]. This highlights that CB1 receptor activity is mediating signaling in the control of neuronal mechanisms underlying CSD.

By modulating the activity of the neuronal network during CSD, the ECS can regulate pain and inflammation [14, 21–23]. In nitroglycerine-induced migraine models, Akerman [24] found that AEA reduces trigeminovascular system excitability, which is implicated in migraine pain generation. Consistent with its anti-nociceptive role, endocannabinoids levels are low in patients with chronic migraine [25]. These findings suggest that active ECS may offer protection against the onset or severity of migraine. Moreover, ECS also participates in modulation of neuroinflammation through inhibition of the activity of enzymes involved in the production of pro-inflammatory signals, reducing the expression of inflammatory molecules such as prostaglandins and leukotrienes [26].

Given the role of ECS in migraine and pain, enhancing endocannabinoids is a promising tool to exert therapeutic effects on pathological neuroinflammation and hyperexcitability. Inhibiting endocannabinoids degradation is one of the most obvious tools to enhance endocannabinoids effects. The two main endocannabinoids are AEA and 2-arachidonoylglycerol (2-AG). AEA is degraded by FAAH (fatty acid amide hydrolase) [27] and 2-AG by MAGL (monoacylglycerol lipase) [28] and ABHD6 (alpha/beta-hydrolase domain containing 6) [29]. Importantly, inhibition of 2-AG and AEA hydrolysis also exerts anti-inflammatory and neuroprotective effects, by preventing the formation of the degradation product arachidonic acid, and thus the downstream synthesis of proinflammatory prostaglandins [30]. The activity of MAGL and FAAH differs in several areas involved in migraine signaling [31]. We previously found high FAAH activity in rat and human dura, where AEA is substantially lower compared to 2-AG [32]. Vice versa, in the trigeminal ganglia, there is higher MAGL activity [32]. In cortical areas, where CSD develops, both MAGL and FAAH are similarly active [31]. Given the different activity of FAAH and MAGL in several areas involved in migraine pain signaling, an effective inhibition of both would likely be needed to achieve migraine analgesia. Interestingly, ABHD6 was recently found to be expressed in brain microglia and neurons [33], which offers additional targets for enhancing endocannabinoid signaling. AKU-005 was previously reported as a potent endocannabinoid hydrolase inhibitor [14, 34]. AKU-005 was shown to reduce hyperalgesia in the nitroglycerin mouse model of migraine, without corresponding changes in endocannabinoid or related lipid levels in the examined regions, suggesting that the observed behavioral effects were likely not mediated by the endocannabinoid system [35]. In the present study, we investigated the ability of AKU-005 to elevate levels of AEA and 2-AG by selectively inhibiting multiple hydrolyzing enzymes in occipital cortex slices from rats and mice, areas not previously studied in this context. Furthermore, we assessed interspecies variability in the cortical inhibition of MAGL, FAAH, and ABHD6, aiming to better characterize how AKU-005 interacts with the ECS. Finally, we correlated these molecular effects with a corresponding reduction in ex vivo cortical CSD following AKU-005 pre-treatment.

Materials and methods

Animals

P24-P26 male outbred Wistar rats (Envigo Laboratories B.V., The Netherlands) were delivered to the Lab Animal Centre of University of Eastern Finland. After 2-weeks of quarantine, rats were used at P38-P40 for experimentation. We selected this age for rats to ensure comparability with our previous study [32]. Male C57 BL/6 J-OlaHsd mice 10–12 months old and C57 BL/6 J-Jax mice 2–4 months used for this study were produced

and maintained in the animal facility of the University of Eastern Finland. Mice strains and ages were not specifically chosen for this study. These animals were originally purchased for other projects where the brain was not required. To minimize unnecessary animal use and reduce costs, we included their brains in this study rather than acquiring additional animals. Importantly, we did not observe any strain- or age-related differences in our data. The number of rats and mice used in this study is indicated in the figure legends as "n" for each experiment. Multiple slices were obtained from a single rat or mouse cortex to conduct various experiments included in this paper. Animals were housed under the following conditions: 12-h dark/light cycle, grouped housing, ad libitum access to food and water, ambient temperature of 22 °C. All experimental procedures performed in this study follow the rules of the European Community Council Directive of September 22, 2010 (2010/63/EEC). The Animal Care and Use Committee of the University of Eastern Finland (license EKS- 008–2019 for rats and license EKS-005–2022 for mice) approved all experimental protocols.

Cortical slices preparation

Our ex vivo slice model preparation is partially based on the one described by Tang et al. [36]) and Vitale et al. [37], with adaptations to suit our experimental setup for live calcium imaging. In this study, the brains from rats and mice were resected in the animal facility, and transported in aCSF (125 mM NaCl, 3.5 mM KCl, 1.25 mM NaH2PO4, 2 mM CaCl2, 1.3 mM MgSO4, 25 mM NaHCO3, and 10 mM D-Glucose) in ice to the laboratory. Whole brain was left in oxygenation in aCSF for 20 min. The brain was then placed in a mold with low melting point Agarose 2%. Mouse coronal cortical slices (350 µm) were obtained using a Vibratome (Campden Model 7000 smz- 2), slicing ad 0.08 µm*sec^{-1}. From each slice, the cortical portion was isolated and placed in oxygenation in aCSF for 20 min recovery before treatments. Afterwards, slices were split in 4 h pre-incubation with AKU-005 100 nM or in control condition aCSF + DMSO. One slice per treatment was used for calcium imaging. The remaining slices were treated ex-vivo with KCl 100 mM (aCSF with compensated osmolarity by reducing NaCl molarity), inducing CSD. Finally, all the slices were frozen for activity-based protein profiling (ABPP) and LC–MS/MS, organized by treatment group and individual mouse. Figure 1 summarizes our experimental flow in a diagram.

Activity-based protein profiling (ABPP)

Tissue samples were mechanically homogenized with a glass homogenizer and a sonicator (5 s sonication repeated five times, with 5 s intervals in-between) in phosphate-buffered saline (PBS). Protein concentrations were determined with bicinchoninic acid (BCA) protein assay, as previously described [38]. ABPP followed an established protocol [39]. In brief, homogenized samples were first diluted in PBS to obtain the desired concentration of 0.2 mg/ml for both mouse and rat cortical samples. Samples were then incubated for one hour either with the vehicle DMSO (control) or with the inhibitor using the following treatments to identify

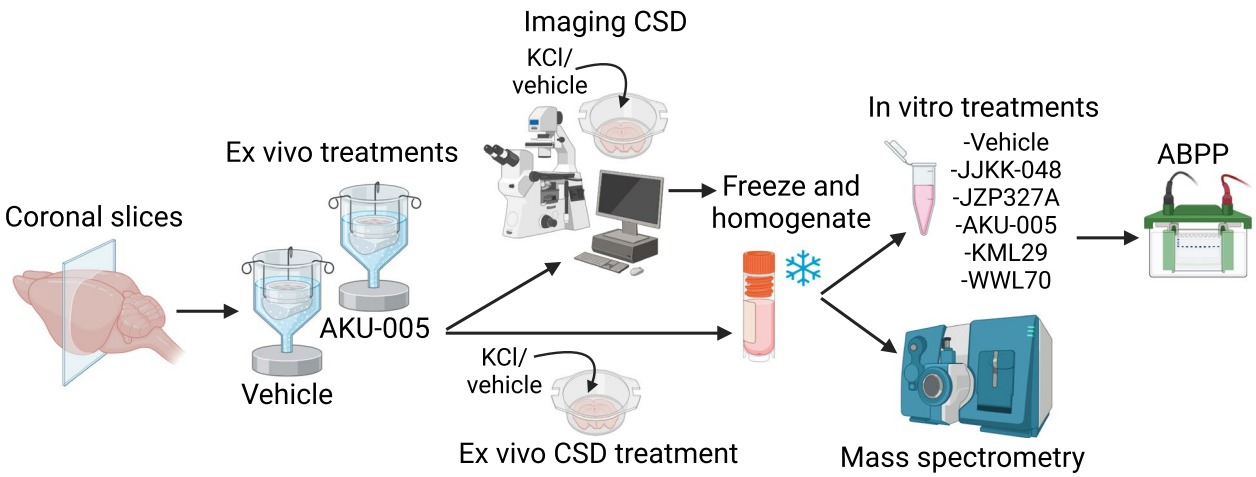

Fig. 1 Schematic of experimental flow for rats and mice cortical slices. Coronal slices of mouse and rat occipital cortex are pre-incubated ex vivo with either a vehicle or AKU-005 (100 nM). For live calcium imaging, one slice per treatment is used and then exposed to either a vehicle or high KCl (100 mM) to induce cortical spreading depression (CSD). The remaining slices undergo the same ex vivo treatments of high KCl or vehicle without imaging. All slices from the same animal and treatment group are then frozen together, homogenized, and divided into two portions. One portion is utilized for activity-based protein profiling (ABPP) assay, during which additional in vitro inhibitory treatments are performed. The remaining homogenized material is analyzed using mass spectrometry

specific enzymatic bands: MAGL/FAAH- inhibitor AKU-005 (100 nM, 500 nM, 1 μM; synthetized in University of Eastern Finland, Kuopio, Finland), FAAH-inhibitor JZP327 A (1 μM; synthetized at University of Eastern Finland, Kuopio, Finland), MAGL-inhibitors KML29 (1 μM; Cayman chemicals) and JJKK- 048 (100 nM; Cayman chemicals, Ann Arbor, MI, USA) and ABHD6-inhibitors WWL70 (1 μM; Cayman chemicals) and JZP430 (1 μM; synthetized at University of Eastern Finland, Kuopio, Finland). After one-hour of pre-incubation with inhibitors/DMSO, the active site serine-targeting fluorescent fluorophosphonate probe TAMRA 1 μM (ActivX Fluorophosphonate Probes, Thermo Fisher Scientific Inc., Rockford, IL, USA) was added to each tube and left in an additional incubation for one hour at room temperature to label remaining active serine hydrolases. The reaction was stopped by adding 2X SDS gel loading buffer. Finally, 10 μl of each sample were loaded per lane for 10% SDS-PAGE electrophoresis (250 mV, 750 mA, 300 s). Running buffer was prepared for each run with cold mQ water and stored overnight in +4 °C. Gel images were acquired by using ChemiDocTM MP Imaging System (BIO-RAD Laboratories, Hercules, CA, USA) with Cy3 blot application (602/50, Green Epi, Manual Exposure 30–420 s). Quantification of bands was analyzed using the ImageLab software (BIO-RAD Laboratories).

Mass spectrometry analysis of endocannabinoids

Detailed descriptions of sample preparation and instrumental parameters for the analysis of endocannabinoids levels have been previously provided [40]. For the preparation, desired volume of the homogenized sample (30–50 μl) was transferred to a tube. To each sample, 500 μl ice cold methanol, 50 μl AEA-d8 internal standard, and 50 μl 2-AG-d8 internal standard were added. Tubes were vortexed for one minute each and then placed in sonicator bath for 30 s. Ice cold mQ water in a volume equal to (500 μl – transferred volume of the sample) was used to wash each 1.5 ml tube, ice cold chloroform was added and mixed. After centrifugation at 1500 g for 10 min at +4 °C, the lower layer of chloroform was removed and transferred to a new glass tube. This process was repeated twice. Glass tubes with chloroform were transferred to drying with nitrogen gas flow. After evaporation, 50 μl acetonitrile were added in each glass tubes and left in incubation for 10 min at room temperature with 1 min vortexing every 2 min. Samples were measured with a reversed phase liquid chromatography technique coupled with the triple quadrupole mass spectrometry (LC–MS/MS), operating in multiple reaction monitoring scanning (MRM). LC–MS/MS analysis was performed using Agilent Technologies 6410 triple quadrupole mass spectrometer coupled to Agilent Technologies 1200 series HPLC system. Separation was achieved using Zorbax Eclipse XDB-C18 (Agilent Technologies) column with an isocratic method. The flow rate was 0.5 ml/min, and the total run time was 4 min. The mass spectrometer was operated in positive ion mode using MRM for quantification of the analytes. Deuterated internal standards (AEA-d8 and 2-AG-d8) were used for quantification. This method is selective, precise, and accurate for concentrations within a range of 0.4–70 nM for N-acylethanolamines and 40–11,000 nM for 2-AG. AEA and 2-AG concentration (pM/ng) were calculated according to protein concentration (mg/ml) of each sample.

Fluorescent glycerol assay

Inhibition and selectivity of AKU-005 against human and mouse MAGL and ABHD6 was measured with a sensitive fluorescence-based assay in a 96-wellplate format, essentially as previously reported [39]. For ABHD6 activity, lysates of HEK293 cells transiently expressing human or mouse ABHD6 were used, and for MAGL activity, stably expressing 3HA-tagged human MAGL or transiently expressing mouse MAGL were used [39, 41]. Mock-transfected HEK- 293 cells were used to control background signaling as previously described [39]. Briefly, glycerol production, which is coupled via an enzymatic cascade to generate resorufin, was kinetically monitored for 90 min period at room temperature (with λex 530 nm; λem 590 nm) using a Tecan Infinite M200 plate reader (Tecan Group Ltd., Männedorf, Switzerland). Cell lysates (99 μl, 1–3 μg protein/well) were preincubated for 30 min with the vehicle (DMSO: control) or AKU-005 with the indicated concentrations (1 μl), after which the substrate 1-AG (12.5 μM final concentration) was added (100 μl). The IC_{50}-values were calculated by Graphpad Prism version 5.03 for Windows, GraphPad Software, San Diego, California USA, www.graphpad.com.

Cortical slices calcium imaging

Slices for ex vivo experiments were imaged with 10 ×Objective using Olympus IX- 70 (Tokyo, Japan) equipped with CCD camera (SensiCam, PCO imaging Kelheim, Germany). Setup setting: Binning 1× 1, Loop count calculated as ((cycle minutes* 60) *2), sampling frequency 2 frames per second. Excitation wavelength was set as 495 nm. Rapid Solution Changer RSC200 (Bio-Logic Science Instruments, Grenoble, France) perfusion system allowed to perform protocols involving perfusion of multiple treatments and ensuring a fast perfusion speed of 3 ml/min. After 4 h pre-treatment in AKU-005 (100 nM), each slice was incubated for 20 min with fluorescent probe Fluo- 4+ AKU-005 (100 nM), followed by 20 min resting condition in aCSF +AKU-005 (100 nM) at room temperature. Finally, slices were tested for their

response to KCl 100 mM (simulating CSD) with the following protocol: 2 min Baseline in BS, 5 min KCl 100 mM, and 5 min washout in BS. Only waves with the typical CSD speed of 3–5 mm/min were selected. Due to the experimental setup, where the drug was applied from the top of the slice and recordings were made from the camera below, drug penetration through the slice was necessary to visualize the wave. Since the slice was surrounded by the administered solution, the treatment's effects were more pronounced at the slice margins, which were more readily accessible to the drug.

Recording and post-processing of data was performed with Live Acquisition and Offline Analysis Software (TILL Photonics GmbH, Germany). For response analysis regions of interest (ROIs) were drawn in the area with higher response to KCl. CSD intensity was determined as the highest value of fluorescence intensity, calculated by the formula $\Delta F/F = (F - F0)/F0$, following KCl exposure.

Statistical analysis

Statistical analysis was performed with GraphPad Prizm software (GraphPad Prizm Software, La Jolla, USA). Data were checked for normality distribution (D'Agostino and Pearson test, Anderson–Darling test, Shapiro–Wilk test, and Kolmogorov–Smirnov test) before statistical tests. Data were considered normally distributed when they passed all the tests mentioned above. Either unpaired student T-test and One-Way ANOVA with Tuckey post-hoc test was used for normally distributed data. Non-parametric and Wilcoxon signed-rank test, Mann–Whitney or Kruskal–Wallis with Dunn's post-hoc tests were applied for non-normally distributed data. Statistical significance differences were set accordingly to p-value: * $p < 0.05$, ** $p < 0.01$, *** $p < 0.001$. Statistical outliers of each data group were found with ROUT method and excluded from the analysis. To ensure statistical accuracy and retain comparability, given the mixed nature of the data, comprising both normally and non-normally distributed variables, all these results are presented as median ± interquartile range (IQR).

Results

AKU-005 inhibits MAGL, FAAH, and ABHD6 *ex vivo* in rat cortical slices under physiological and CSD conditions

We first used in vitro treatments to distinguish the activity of MAGL, FAAH and ABHD6 in rat occipital cortex slices using the ABBP activity assay (Fig. 2 A). FAAH activity was inhibited in vitro by JZP327 A, a specific FAAH-inhibitor, and AKU-005 in control and CSD conditions. MAGL was inhibited in vitro by JJKK- 048, a selective MAGL inhibitor, and AKU-005, and ABDH6 activity was inhibited by AKU-005 (Fig. 2 A). MAGL appears in nervous tissues as a double band representing two different isoforms of the enzyme.

The same activity assay was then used to assess the biological effect of the ex vivo treatments of CSD and/or AKU-005 on the activities of MAGL, FAAH and ABHD6 (Fig. 2 A). The activity band densities from Fig. 2 A were quantified (Fig. 2 B-E). The basal activity of FAAH measured in the absence of inhibitors or CSD, was slightly lower than that of MAGL (Fig. 2 B). MAGL quantification reflects the combined intensity of the two bands, as our focus is on total MAGL activity. Both MAGL and FAAH exhibited more than double the activity compared to ABHD6 (Fig. 2 B). Enzyme activities were inhibited in rat cortical slices with AKU-005 ex vivo treatment, followed by high KCl treatment (AKU CSD; Fig. 2 A, C-E). FAAH basal activity used as control (basal) in rat occipital cortex slices remained unchanged under CSD conditions, however AKU-005 ex vivo treatment reduced control FAAH activity from 2 a.u. to 0.6 a.u. (Fig. 2 C). Similarly, FAAH activity during CSD with AKU-005 ex vivo pre-treatment was reduced from 1.7 a.u. to 0.5 a.u. (Fig. 2 C). In Fig. 2 D, MAGL control basal activity (basal) of 2.6 a.u. was slightly increased to 3.2 a.u. during CSD. AKU-005 ex vivo pre-treatment reduced control MAGL basal activity to 0.6 a.u. (Fig. 2 D). Finally, the increase of MAGL activity, that occurred with CSD, was reduced by AKU-005 ex vivo pre-incubation (AKU CSD) to 0.5 a.u. (Fig. 2 D). The basal activity of ABHD6 remained low and unchanged during CSD (Fig. 2 E). However, ABHD6 activity during CSD was reduced from 0.8 a.u. to 0.2 a.u. upon AKU-005 ex vivo pre-treatment (Fig. 2 E).

Using quantitative LC–MS/MS analysis, we also measured 2-AG and AEA levels in the rat cortex slices. In line with the high hydrolases' activity, the levels of AEA and 2-AG were found relatively low in control conditions (basal) with levels of 0.2 pM/ng (AEA) and 0.3 pM/ng (2-AG) (Fig. 2 F and G). In rat cortical slices, CSD induced an increase of AEA levels to 0.3 pM/ng (Fig. 2 F). This is consistent with the fact that FAAH, the enzyme responsible for degrading AEA, does not alter its activity under CSD conditions. With FAAH activity remaining unchanged, there is no compensatory degradation to the elevated AEA levels. AKU-005 ex vivo pre-treatment produced per se an even higher increase of AEA basal levels to 0.6 pM/ng (Fig. 2 F). Additionally, during CSD, AKU-005 triggered higher AEA levels to 0.9 pM/ng (Fig. 2 F). In contrast to AEA, 2-AG levels in control (basal) and CSD remained unchanged (Fig. 2 G), probably due to compensated increase of MAGL degrading activity during CSD (Fig. 2 D). However, in line with decreased MAGL activity, AKU-005 increased 2-AG

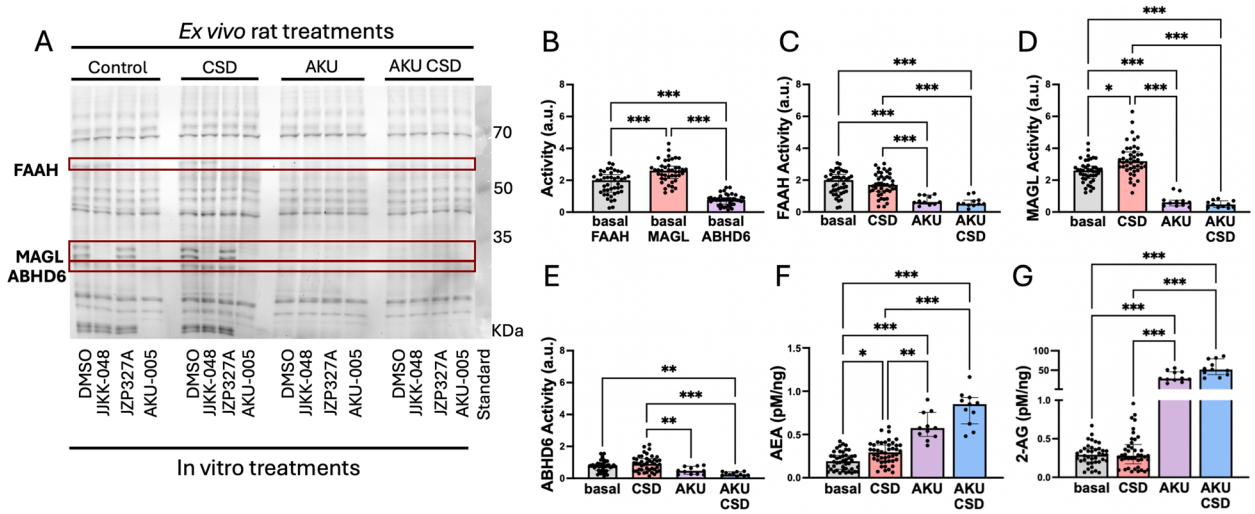

Fig. 2 Profiling serine-hydrolases MAGL, FAAH and ABHD6 activity and endocannabinoid levels in rat cortical samples. **A** Competitive gel-based activity-based protein profiling (ABPP) of MAGL, FAAH and ABHD6 in rat cortical samples. ABPP was performed on frozen rat cortical slices after the following ex vivo treatments: control (basal), high KCl (CSD), AKU-005 (AKU) pre-incubation, AKU preincubation followed by high KCl (AKU CSD). For the ABPP, samples were incubated in vitro for one hour with the vehicle DMSO (basal) and the following treatments to identify specific enzymatic bands: MAGL/FAAH/ABHD6 inhibitor AKU 100 nM, FAAH-inhibitor JZP327 A 1 µM, MAGL-inhibitor JJKK- 048 100 nM; and then labelled with fluorescent probe TAMRA-FP. **B** Basal FAAH activity is slightly lower than MAGL one. ABHD6 basal activity is lower than both MAGL and FAAH basal activities (n = 43, p < 0.001, Kruskal–Wallis with Dunn's post-hoc test). The same basal data in panel B is shown in panels C-E. **C** FAAH basal activity (basal) was unchanged following CSD. FAAH activity levels in AKU condition were reduced compared to the basal ones (n = 43 in basal and n = 11 in AKU, $p = 0.0001$, Kruskal–Wallis with Dunn's post-hoc test). FAAH activity was also reduced in AKU CSD condition compared to CSD ($n = 43$ in CSD and n = 11 in AKU CSD, $p = 0.0001$, Kruskal–Wallis with Dunn's post-hoc test). **D** MAGL basal activity (basal) was increased during CSD ($n = 43$, $p = 0.0145$, Kruskal–Wallis with Dunn's post-hoc test). Compared to basal levels, MAGL activity levels in AKU condition were reduced ($n = 11$, $p = 0.0006$, Kruskal–Wallis with Dunn's post-hoc test). Increased MAGL activity in CSD condition was reduced in AKU CSD condition ($n = 11$, $p < 0.001$, Kruskal–Wallis with Dunn's post-hoc test). **E** ABHD6 basal activity (basal) was unchanged following CSD. ABHD6 activity in CSD condition was reduced in AKU CSD condition ($n = 43$ in CSD and $n = 11$ in AKU CSD, $p < 0.0001$, one-way ANOVA with Tukey post-hoc test). **F** AEA levels increased following CSD ($n = 44$, $p = 0.006$, one-way ANOVA with Tukey post-hoc test). AKU-005 pre-treatment lead to high increase of AEA basal levels (AKU, $n = 11$, $p < 0.001$, one-way ANOVA with Tukey post-hoc test), and AEA levels after CSD (AKU CSD, n = 11, p < 0.001, one-way ANOVA with Tukey post-hoc test). **G** 2-AG basal levels did not change after CSD. AKU-005 pre-treatment increased 2-AG levels in AKU conditions ($n = 39$ for basal and $n = 11$ for AKU, $p < 0.001$, Kruskal–Wallis with Dunn's post-hoc test) and AKU CSD conditions ($n = 41$ for CSD and $n = 11$ for AKU, $p < 0.001$, Kruskal–Wallis with Dunn's post-hoc test)

levels in control conditions from 0.3 pM/ng to 28.7 pM/ng (Fig. 2 G). Under CSD, AKU-005 pre-treatment increased 2-AG levels even higher levels from 0.3 pM/ng to 51.7 pM/ng (Fig. 2 G).

Taken together, ex vivo pre-treatment with AKU-005 reduced MAGL and FAAH activities under basal conditions. Furthermore, during CSD, AKU-005 decreased the activities of MAGL, FAAH, and ABHD6. Notably, AKU-005 also increased 2-AG and AEA levels under both physiological and CSD conditions.

AKU-005 inhibits MAGL *ex vivo* in mouse cortical slices under CSD state

Similarly to rats, MAGL, FAAH and ABHD6 activities were next assessed in mouse occipital cortex slices with ABPP approach (Fig. 3). In the same setting, in vitro treatments were used for specifically identifying the hydrolases bands (Fig. 3 A). In particular, JZP327 A is a specific FAAH inhibitor, KML29 is a MAGL inhibitor, WWL70 and JZP430 an ABHD6 inhibitors. Additionally, AKU-005 has been also tested in vitro, being our experimental inhibitor. Due to the generally lower activity of endocannabinoid hydrolases in mouse cortex (Fig. 3 A), additional ABHD6 inhibitors were included in comparison to the rat ABPP to accurately identify the targets, even with reduced band intensity.

The activity bands of Fig. 3 A have been quantified, and their values have been represented in Fig. 3 B-E. In general, FAAH and MAGL activities were found lower in mice (Fig. 3 B) compared to rat tissue (Fig. 2 B). FAAH activity was barely detectable in mouse cortex slices (0.6 a.u., Fig. 3 B) and lower than MAGL basal activity (2 a.u., Fig. 3 B). Instead, ABHD6 activity in mouse cortical slices (0.8 a.u., Fig. 3 B) was found comparable to the one in the rat cortical slices (Fig. 2 B). MAGL activity was reduced during CSD from 3 a.u. to 0.8 a.u. (Fig. 3 D) after AKU-005 ex vivo pre-treatment. However, neither FAAH (Fig. 3 C) nor ABHD6 (Fig. 3 E) were inhibited by

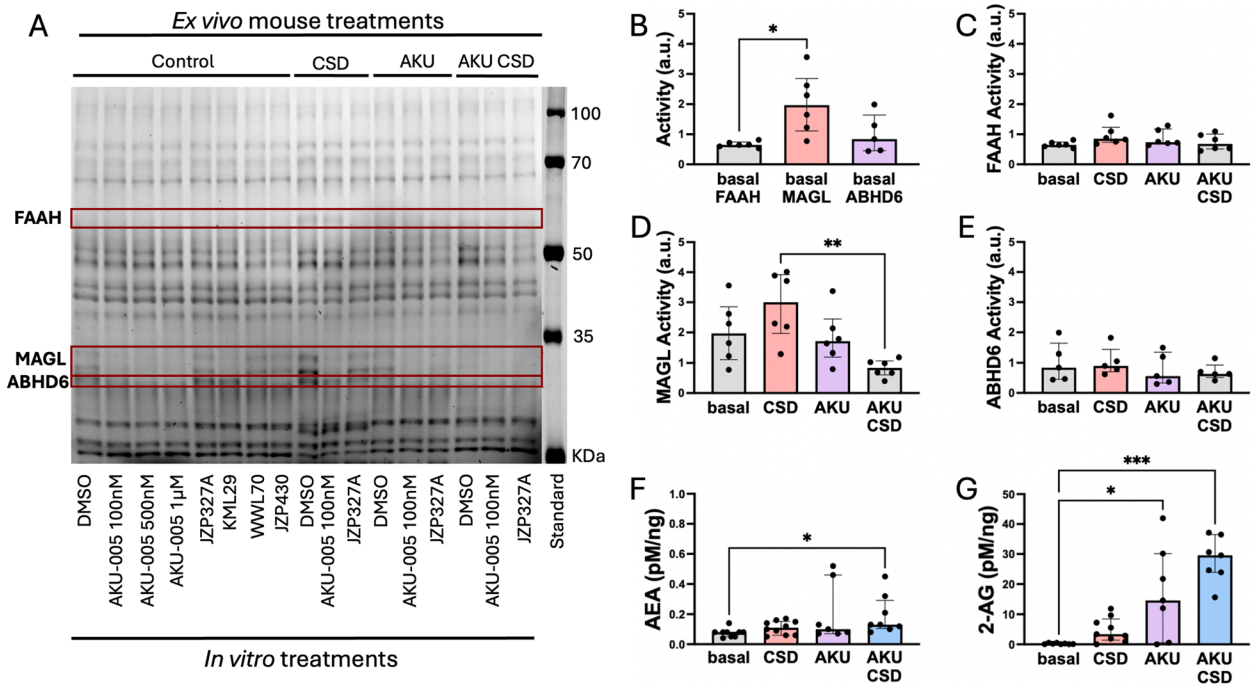

Fig. 3 Profiling serine-hydrolases MAGL, FAAH and ABHD6 activity and endocannabinoids levels in mouse cortical samples. **A** Competitive gel-based activity-based protein profiling (ABPP) of MAGL, FAAH, and ABHD6 in mouse cortical samples. ABPP was performed on frozen mice cortical slices after the following ex vivo treatments: control (basal), high KCl (CSD), AKU-005 (AKU) preincubation, AKU preincubation followed by high KCl (AKU CSD). For the ABPP, samples were then incubated in vitro for one hour with the vehicle DMSO (basal) and the following treatments to identify specific enzymatic bands: dual MAGL/FAAH inhibitor AKU (100 nM, 500 nM, 1 µM), FAAH-inhibitor JZP327 A 1 µM, MAGL-inhibitor KML29 1 µM, ABHD6-inhibitors WWL70 1 µM and JZP430 1 µM; and then labelled with fluorescent probe TAMRA-FP. Complete description of the procedure in Material and Methods. **B** The basal activity of FAAH is lower than that of MAGL. **C** FAAH activity was not significantly changed in the 4 tested conditions ($n = 6$). The same basal data in panel B is shown in panels C-E. **D** MAGL activity in CSD condition was reduced in AKU CSD condition ($n = 6$, $p = 0.003$, Kruskal–Wallis with Dunn's post-hoc test). **E** ABHD6 activity was not significantly changed in the 4 tested conditions ($n = 5$). **F** AEA levels were not affected by any ex vivo treatment of the cortical slices ($n = 7$) **G** 2-AG levels were increased after AKU preincubation, both in basal conditions ($n = 7$, $p = 0.003$, Kruskal–Wallis with Dunn's post-hoc test) and during CSD ($n = 7$, $p < 0.001$, Kruskal–Wallis with Dunn's post-hoc test)

ex vivo AKU-005 application under either basal or CSD conditions. The lack of inhibition of FAAH and ABHD6 in the mouse cortex ex vivo may be partially attributed to their low basal activity, which leaves limited potential for further inhibition. Additionally, the potency of AKU-005 may vary between species due to differences in their endocannabinoid system profiles and pharmacokinetics. The power of inhibition by AKU-005 may be increased by a higher compound concentration and/or an increased n-number of mice.

Consistently to the ABPP outcome, results from LC–MS/MS showed that while AEA levels remained unchanged (Fig. 3 F), 2-AG levels were largely increased after AKU-005 ex vivo pre-incubation during CSD from 3.4 pM/ng to 29.6 pM/ng (Fig. 2 G). Unexpectedly, regardless of a lack of MAGL inhibition by AKU-005 in basal (control) conditions, there was an increase in 2-AG levels from 0.1 pM/ng to 14.6 pM/ng (Fig. 2 G). Although AKU does not inhibit basal MAGL enzymatic activity directly, it may have subtle off-target effects that indirectly increase 2-AG levels also under physiological conditions.

In summary, the ex vivo inhibitory effect of AKU-005 at 100 nM concentration was weaker in mouse cortical slices than in rats. This effect in mice cortex primarily involved a decrease in MAGL activity under CSD conditions and a corresponding increase in 2-AG levels.

In vitro inhibitory effect of AKU-005 on FAAH, MAGL and ABHD6 in rat and mouse

Next, a general inhibitory efficiency of AKU-005 against endocannabinoids hydrolases in rat and mouse cortical slices was evaluated from the in vitro treatments. For instance, we assessed the inhibitory effect of AKU-005 on the same slices used in Figs. 2 and 3, but this time in vitro, following freezing and homogenization (treatments indicated on the bottom sides of the gels in Fig. 2 A and Fig. 3 A). Basal levels of FAAH, MAGL, and ABHD6 activities

were set at 100%, and the percentage of inhibition by AKU-005 was then calculated based on its own control.

In rats, the in vitro analysis of AKU-005 confirmed its triple inhibitory activity, which was previously observed ex vivo. Indeed, we found that AKU-005 (100 nM) almost completely inhibited the activity of FAAH and MAGL in rat cortical slices. Indeed, both FAAH and MAGL activity were reduced by 79% (Fig. 4 A and B). Moreover, this treatment had also a moderate inhibitory effect on ABHD6 activity resulting in 30% decrease of its activity (Fig. 4 C).

Unlike rat cortical tissue, in mouse cortical slices, the endocannabinoids hydrolyzing activity of FAAH and ABHD6, could not be blocked in vitro by AKU-005 (Fig. 4 D, 4 F), confirming also in this case the previously described ex vivo outcome. However, differently from the ex vivo treatment, AKU-005 exhibited a partial but significant inhibition of basal mouse MAGL activity at all used concentrations: 56% at 100 nM, 62% at 500 nM, and 51% at 1 µM (Fig. 4 E). This suggests that AKU-005 has the potential to inhibit MAGL in the mouse cortex as well. Achieving an ex vivo effect may require either a higher concentration or improved drug penetration to reach the targets.

To determine whether AKU-005 could function as a multiple inhibitor in other species as mice and humans, or if its effect is limited to rats, we tested its inhibition and selectivity against mouse and human MAGL and ABHD6, using lysates from HEK293 cells overexpressing these enzymes. Indeed, as shown in Fig. 5, we confirmed that AKU-005 can also inhibit ABHD6, although less potently than MAGL. Interestingly, AKU-005 appeared more selective for mouse MAGL (mMAGL) and ABHD6 (mABHD6) over the human enzymes (hMAGL and hABHD6), showing equal potency for ABHD6 in both species (Fig. 5 B) but higher potency for inhibiting mouse MAGL compared to human MAGL (Fig. 5 A). The specific values for inhibition potency of mouse and human MAGL and ABHD6 are shown in Fig. 5 C. It has not been practical to evaluate AKU-005's inhibition of FAAH using the same glycerol assay. This is because monoacylglycerols, such as 2-AG and its isomer 1-AG (commonly used in this assay), are suboptimal substrates for FAAH. Under physiological conditions, FAAH primarily degrades AEA. Due to these observations, we see AKU-005 as a potential multiple inhibitor of MAGL, FAAH and ABHD6 in different species.

Overall, AKU-005 shows potential as a triple inhibitor of FAAH, MAGL, and ABHD6. However, its inhibitory

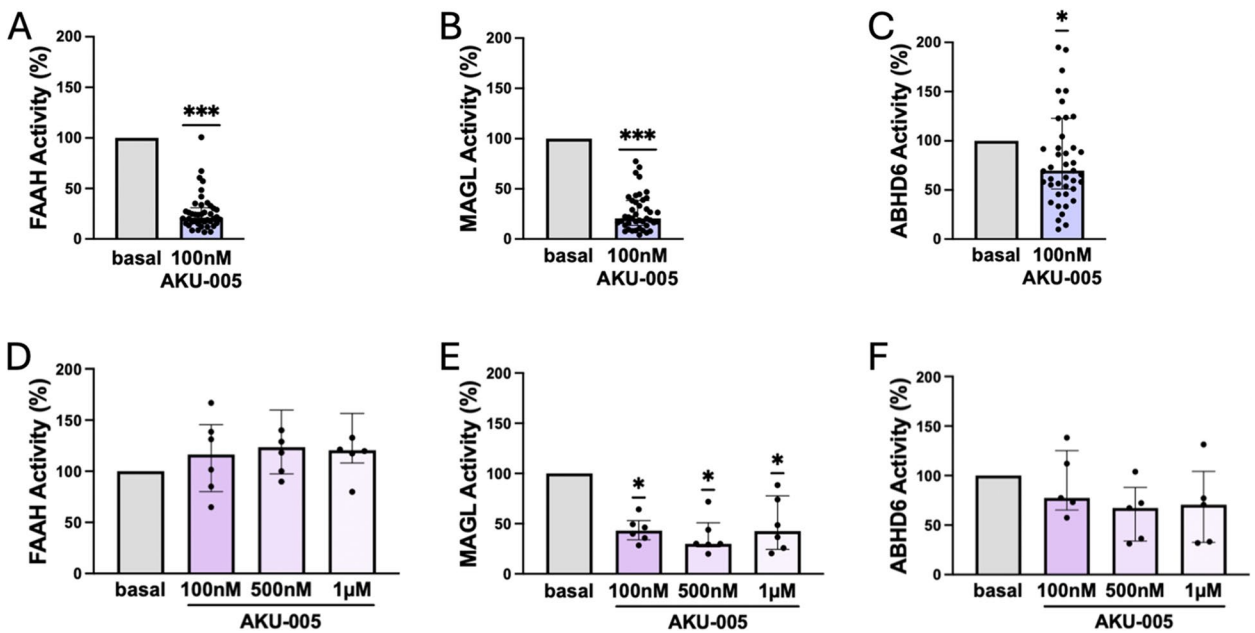

Fig. 4 Blocking capacity of the inhibitor AKU-005 on rat and mouse enzymes FAAH, MAGL and ABHD6. Data are from ABPP testing of rat and mouse cortical slices. Samples were incubated in vitro for one hour with the vehicle DMSO (basal) and inhibitor AKU-005 (AKU) 100 nM for rat samples and at different concentrations (100 nM, 500 nM, 1 µM) for mouse samples. **A** AKU (100 nM) strongly inhibited FAAH activity in rat samples ($n = 42$, $p < 0.0001$, Wilcoxon signed-rank test). **B** AKU (100 nM) strongly inhibited MAGL activity in rat samples ($n = 42$, $p < 0.0001$, Wilcoxon signed-rank test). **C** AKU (100 nM) slightly inhibited ABHD6 activity in rat samples ($n = 43$, $p = 0.05$, Wilcoxon signed-rank test). **D** AKU did not reduce FAAH activity in mouse samples ($n = 6$). **E** AKU reduced MAGL activity in mouse samples ($n = 6$, $p = 0.0001$ at 100 nM, $p = 0.031$ at 500 nM, $p = 0.006$ at 1 µM, Wilcoxon signed-rank test). **F** AKU did not reduce ABHD6 activity in mouse samples at any concentration ($n = 5$)

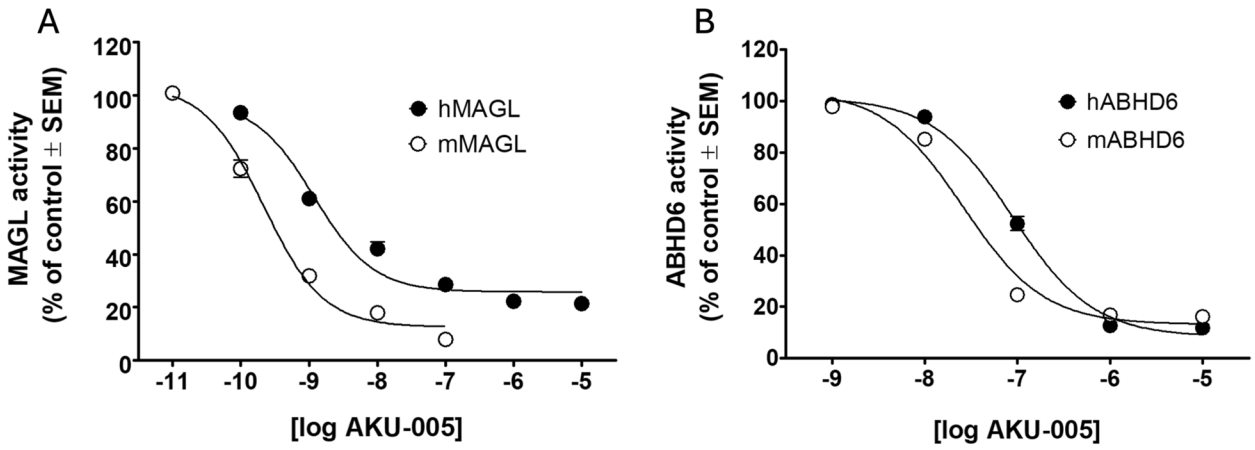

C

Serine hydrolase	Log [IC_{50}] ± SEM	IC_{50}
hMAGL	-8.93 ± 0.11	1.2 nM*
mMAGL	-9.66 ± 0.08	0.22 nM*
hABHD6	-7.05 ± 0.05	89 nM*
mABHD6	-7.58 ± 0.09	26 nM*

Fig. 5 Inhibitor activity of AKU-005 against mouse and human MAGL and ABHD6 tested in a glycerol assay. **A** Dose-dependent inhibition by AKU-005 on human (h) and mouse (m) MAGL enzyme. **B** Dose-dependent inhibition by AKU-005 on human and mouse ABHD6 enzymes. The enzymes were overexpressed in HEK293 cells and lysates were processed as described in Methods. The data are from at least three independent experiments performed in duplicate. **C** Table with Log IC_{50} and IC_{50} values of AKU-005 for inhibiting human (h) and mouse (m) MAGL and ABHD6. The results were obtained by testing AKU-005 in MAGL- and ABHD6-overexpressing HEK293 cell preparations in a sensitive glycerol assay, as described in methods. An asterisk (*) denotes a statistically significant difference between the IC_{50} values of hMAGL and mMAGL (two-way paired t-test, $p = 0.0012$). The data are from at least 3 independent experiments

effect appears to be species-specific in the rat and mouse cortex, acting as triples inhibitor for rats and MAGL-inhibitor for mice. This differential effect is likely influenced by the basal endocannabinoid system profile and the pharmacokinetics of AKU-005 in each species within this specific region.

Species-specific AKU-005 inhibition of endocannabinoid hydrolases reduces CSD

Finally, we tested in rat and mouse occipital cortex slices, the ex vivo pre-treatment effect of AKU-005 (AKU) on CSD induced by application of 100 mM KCl. In both rats (Fig. 6 A) and mice (Fig. 6 B) ex vivo cortical slices CSD wave propagated with rate of 3–5 mm/min typical for the CSD phenomenon [42]. The intensity of the wave was quantified at the margins of the cortex, where the effect was more pronounced (indicated by the red circle in Fig. 6 A and Fig. 6 B). Notably, the intensity of the CSD wave detected in control and AKU-005 pretreated slices was different in rats and mice. Indeed, in rats, the calcium imaging fluorescent traces show a visible decrease in fluorescence average between the control and AKU-005 pre-treated slices (Fig. 6 C and 6 D). Instead, in mice, this major difference is missing (Fig. 6 E and 6 F).

In rat slices, ex vivo CSD intensity was reduced from 60.6% to 31.5% upon 4 h AKU-005 pre-treatment (Fig. 6 G). In line with the signal intensity reflecting the amplitude of the ex vivo CSD wave, AKU-005 pretreatment also significantly decreased the CSD AUC from 96.3 to 48.4 (Fig. 6 H).

Differently from the rat slices, in mice, no change was detected for the ex vivo CSD wave intensity after AKU-005 preincubation, as the amplitude of the CSD-induce calcium signal remains the same between control and AKU-005 pretreatment (Fig. 6 I). However, the AUC was reduced significantly also in mice (from 109 to 75.6; Fig. 6 L). Indeed, the average decay of the CSD-induced calcium signal appears faster in slices pretreated with AKU-005, as evidenced by a sharper decline in the curve following the peak.

Overall, the pretreatment with AKU-005 effectively reduced ex vivo CSD in rat cortical slices, while its

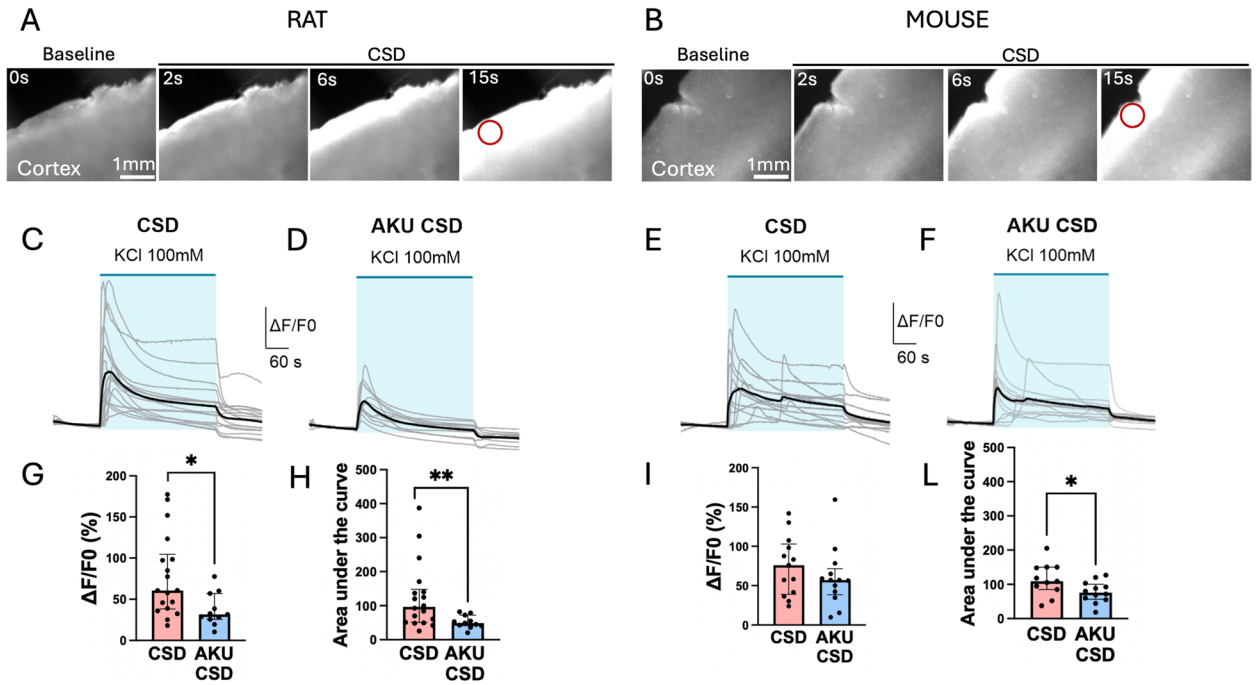

Fig. 6 CSD calcium transients induced by KCl in rat and mouse cortical slices. Slices were incubated for 4 h with DMSO (control) or AKU-005 (AKU) 100 nM (pretreatment), each slice was then incubated for 20 min with fluorescent probe Fluo- 4, followed by 20 min resting condition in aCSF at room temperature. After this, slices were tested in their response to KCl 100 mM. Protocols applied are described in detail in Material and Methods section. **A** and **B** Fluorescence snapshot of rat and mouse cortical slices at 0, 2, 6, 15 s post KCl 100 mM perfusion. Scale bar is 1 mm. **C** Rat cortical slices, calcium fluorescence time series of DMSO pre-incubation control condition. Black trace is representative of the statistics, all other traces are shown in grey. **D** Rat cortical slices, calcium fluorescence time series of AKU 100 nM pre-incubation condition. Black trace is representative of the statistics, all other traces are shown in grey. **E** Mouse cortical slices, calcium fluorescence time series of DMSO pre-incubation control condition. Black trace is representative of the statistic, all other traces are shown in grey. **F** Mouse cortical slices, calcium fluorescence time series of AKU 100 nM pre-incubation condition. Black trace is representative of the statistics, all other traces are shown in grey. **G** Statistical comparison of intensity of fluorescence (ΔF/F0(%)) of KCl-triggered CSD in rat cortical slices. CSD fluorescence intensity was reduced upon 4 h AKU pretreatment ($n = 18$ in CSD and $n = 11$ in AKU CSD, $p = 0.015$, Mann–Whitney test). **H** Statistical comparison of the area under the curve (AUC) of KCl-triggered CSD in rat cortical slices. AKU-005 pretreatment significantly decreases the CSD AUC ($p = 0.007$, Mann–Whitney test). **I** Statistical comparison of intensity of fluorescence (ΔF/F0(%)) of KCl-triggered CSD in mouse cortical slices. Changes in CSD fluorescence intensity were not detected after AKU preincubation ($n = 13$). **L** Statistical comparison of the AUC of KCl-triggered CSD in mouse cortical slices. AKU-005 pretreatment reduced the CSD AUC ($p = 0.040$, Unpaired t-test)

modulation in mice appears more limited. This was in line with the previously observed differential effects of AKU-005 in inhibiting serine hydrolases and enhancing endocannabinoids more strongly and widely in rats (Fig. 2) than in mice cortical slices (Fig. 3).

Discussion

We and others [29, 32, 40] have previously described AKU-005 as a double MAGL and FAAH inhibitor designed to enhance the tone of endocannabinoids. Indeed, given the high complimentary activity of MAGL and FAAH at the cortices in rats [31], the use of an inhibitor, which can target at least these two enzymes already offers a broader efficacy and increased efficiency than mono-targeted drugs. Further exploring the therapeutical potential of this compound, here we present, for the first time, that AKU-005 inhibits three key endocannabinoid-degrading enzymes, MAGL, FAAH and ABHD6, with the resultant desired enhancement of key endocannabinoids in the occipital cortex of rats. The inhibition of these serine hydrolases reduced CSD in cortical brain slices, a model which we used to mimic a classical phenomenon of CSD known to be linked to migraine with aura. Indeed, we found that AKU-005 even at nanomolar concentrations can decrease the intensity of ex vivo CSD waves (with a lower peak of calcium wave and area under the curve) in rats. This observation aligns with previous research indicating the suppression of migraine CSD through direct activation of CB1 receptors [20]. Additionally, our findings support previous work showing that MAGL inhibition by MNJ110 reduces periorbital allodynia in rat CSD models induced by cortical high KCl injection [43]. In mice, AKU-005 inhibited only MAGL, leading to an increase in 2-AG levels under

ex vivo CSD conditions. As a result, the intensity of the CSD-induced calcium wave remained unchanged with AKU-005 pretreatment, but the decay time was modestly shortened.

The differential functional reduction of the ex vivo CSD in rats and mice cortical slices by AKU-005 was consistent with their distinct ECS profiles. Although the 2-AG appears in our results to be predominantly increased over AEA by AKU-005 in both mice and rats during ex vivo induction of CSD in cortical slices, the specific cannabinoid receptor responsible for this remains uncertain and needs further investigation. However, the abundance of CB1 receptors in the brain makes them a likely primary effector of AKU-005 action to reduce pathologically enhanced cortical excitability predisposing to CSD. These inhibitory receptors are also an attractive target for migraine treatment, blocking not only peripheral but also central nociceptive traffic in this disorder.

Targeting CB2 receptors in immune and glial cells may be a complimentary approach to reduce the inflammatory component and chronification associated with severe forms of migraine [15].

For instance, microglia exhibit a much higher capacity to secrete 2-AG compared to astrocytes and neurons [44], suggesting their important role in control of CSD initiation [45]. However, the CSD-induced endocannabinoid release in our ex vivo cortical slice model is primarily driven by astrocytes and neurons, and CB1 agonists but not CB2 agonists have been shown to suppress CSD [20]. However, it is important to keep in mind the previous finding that ABHD6 is expressed and is active in microglia [33], which could open the rout to a new target for AKU-005.

In line with the growing interest in medications targeting receptor heteromers, studies utilizing bivalent CB1 antagonists specifically affecting dimerized CB1 receptors have shown promising pain-alleviating effects [46]. Overall, the di- and oligomerization of G protein-coupled receptors (GPCRs) within the central nervous system (CNS) present attractive therapeutic targets in pain conditions [47, 48]. Beside the canonical cannabinoid receptors, there is also evidence of a possible interaction between CB1 and NMDA receptors [49], which are fundamental for CSD generation and propagation [50]. In line with this, enhancement of endocannabinoids can reduce the activity of NMDA receptors [51].

Finally, our study demonstrates that AKU-005 is a potential multiple inhibitor of MAGL, FAAH, and ABHD6, key enzymes involved in the breakdown of endocannabinoids. In the rat cortex, AKU-005 acts as a triple inhibitor at a concentration of 100 nM, but in mice, only MAGL is inhibited. This is in line with their different endocannabinoids hydrolases profiles. To fully explore its potential across species, higher concentrations or alternative penetration methods should be tested in mice and humans, as AKU-005 was found in this study able inhibit at least both MAGL and ABHD6 enzymes when overexpressed in transfected cells. Evaluating AKU-005's inhibition of FAAH using the glycerol assay has proven impractical. This is due to the fact that monoacylglycerols like 2-AG and its isomer 1-AG, which are typically used in this assay, are not ideal substrates for FAAH. Under normal physiological conditions, FAAH mainly degrades AEA. However, AKU-005 had been previously described to inhibit rat and human FAAH with IC_{50} values of 63 ± 8 nM and 389 ± 65 nM, respectively [24]. It remains unknown whether the same FAAH inhibition observed in rats and humans stands in mice as well. Additionally, the endocannabinoids hydrolase activity profile varies across tissues involved in migraine nociceptive signaling [31], which may affect AKU-005's inhibitory efficacy. Even though an inhibitory effect has not been observed in the cortex, we cannot exclude its efficacy on different tissues. There is a widening knowledge on endocannabinoids enhancement in peripheral areas of the trigeminovascular system, triggering migraine. Indeed, we have recently shown that AKU-005 inhibits meningeal nociceptive spiking [32] and it has also been proved able to reduce trigeminal hyperalgesia in rat nitroglycerine migraine model [35]. Moreover, many other inhibitors of this class have been tested for their analgesic effect at the level of the trigeminovascular system or on migraine related animals' behavior (reviewed in Della Pietra [14]). While we have observed similarities in the endocannabinoid hydrolase profile between rat and human meninges [31], it remains unclear whether this holds true for other migraine-signaling regions or how it compares to the profile in mice. Moreover, little is known about the power of the newly developed endocannabinoids hydrolase inhibitors in the CNS and in counteracting CSD hyperexcitability in migraine with aura. Liktor-Busa [43] proposes an inhibition of either MAGL or ABHD6 to reduce cephalic allodynia in CSD rat models. Consistently with these previous data and based on our recent findings of the high activity of MAGL and FAAH in the highly excitable occipital rat cortex [31], we showed that ex vivo CSD can be reduced by the AKU-005 triple inhibition of MAGL, FAAH, and ABHD6 in cortical slices of rats.

Limitations and future directions

Our current study has some limitations. Male animals were exclusively used to eliminate the confounding effects of fluctuating sex hormones, which are known to influence spreading depolarization responses [52, 53].

There is currently no widely accepted ex vivo model for migraine-related CSD. However, researchers have

explored slice models to better study this complex phenomenon under controlled conditions [36, 37, 54]. While our mouse model presents physiological, anatomical, and cellular differences from humans, the basic mechanisms of this phenomenon are most likely universal. Therefore, our results, showing that AKU-005 attenuates CSD in ex vivo model, suggests inhibitory action of endocannabinoids on ex vivo CSD induction and propagation mechanisms. Given these findings, future studies using established in vivo CSD models [55] will be important to further explore AKU-005's potential to reduce CSD and extrapolate these data to patients with migraine with aura.

The focus of this paper is on the inhibition of MAGL, FAAH, and ABHD6. However, the effectiveness of AKU-005 as a potential therapeutic must be carefully balanced for its effect on other enzymes and considered for their species- and tissue-specificity. Indeed, unlike in mouse brain samples (Fig. 3 A), in rat samples (Fig. 2 A), AKU-005 was found to inhibit, at the studied concentration of 100 nM, two smaller serine hydrolases, which according to our previous research are lysophospholipases A1/A2 (LYPLA1/2; also known as acyl-protein thioesterases 1/2 or APT1/APT2) [56]. Translating our results into migraine patients with aura will require further *in-vivo* pharmacokinetic studies to determine the selectivity of AKU-005 in human tissues.

Conclusion

In summary, we show here that AKU-005 is a triple inhibitor of MAGL, FAAH and ABHD6 that exerts a species-specific reduction in the activities of these enzymes in the occipital cortex of rats and mice. Overall, it exerts a stronger effect on reducing all the three enzymes activity in rats' cortical slices, while inhibiting selectively MAGL during ex vivo CSD in mice cortical slices. AKU-005 also causes a reduction in ex vivo CSD, with a more pronounced effect observed in rat cortical slices compared to mice. Given the known antinociceptive action of cannabinoids, our results suggest a multicomponent therapeutic effect of AKU-005 in alleviating migraine via modulation of the ECS, particularly in conditions associated with CSD, a phenomenon typical of migraine with aura.

Abbreviations

AUC	Area under the curve
2-AG	2-Arachidonoilglycerol
ABHD6	Alpha/beta-hydrolase domain containing 6
ABPP	Activity-based protein profiling
aCSF	Artificial cerebrospinal fluid
AEA	Anandamide
BCA	Bicinchoninic acid
BS	Basic solution
CNS	Central nervous system
CSD	Cortical spreading depolarization
CSF	Cerebrospinal fluid
ECS	Endocannabinoids system
FAAH	Fatty acid amide hydrolase
GPCRs	G protein-coupled receptors
LC–MS/MS	Liquid chromatography technique coupled with the triple quadrupole mass spectrometry
MAGL	Monoacylglycerol lipase
MRM	Multiple reaction monitoring scanning
ROIs	Regions of interest

Supplementary Information

The online version contains supplementary material available at https://doi.org/10.1186/s10194-025-02030-2.

Supplementary Material 1. Reviewer Report.

Acknowledgements

We would like to thank Jayendra Z. Patel for synthetizing JZP- 327 A and Taina Vihavainen for her help with the LC-MS/MS sample preparation. We thank Biocentre Finland and Biocentre Kuopio for their support of the LC-MS laboratory facility. We thank Dr. Else Tolner for her support on the CSD data characterization during the rebuttal phase. Fig 1 has been created with Biorender.com (agreement number UF27 TM9XJW).

Authors' contributions

ADP, RG, JS, and TM supervised the project. ADP, FB, and KI performed ABPP, and calcium imaging and FB and KI analyzed the results. ML, ADP, FB, and KI carried out liquid chromatography coupled with triple quadrupole mass spectrometry and analyzed the results. AA did the glycerol multi-well plate assay. RG managed the mice and helped with tissue collection. FB, KI, and ADP performed statistical analysis. FB and ADP made the figures. FB and ADP wrote the original draft of the manuscript. All authors reviewed and approved the manuscript.

Funding

This work was supported by 2019 Migraine Research Foundation Impact Award to RG and JS. FB was supported by ERASMUS internship program. ADP was supported by the Doctoral Program in Molecular Medicine (DPMM) of the University of Eastern Finland and by OLVI-säätiö (2021). KI was supported by the Finnish National Agency for Education (EDUFI).

Data availability

The datasets used and/or analyzed during the current study are available from the corresponding author on reasonable request.

Declarations

Ethics approval and consent to participate

All experimental procedures performed in this study follow the rules of the European Community Council Directive of September 22, 2010 (2010/63/EEC). The Animal Care and Use Committee of the University of Eastern Finland (license EKS- 008–2019 for rats and license EKS- 005–2022 for mice) approved all experimental protocols.

Consent for publication

Not applicable.

Competing interests

ADP and RG are members of the editorial board of *The Journal of Headache and Pain*, but they were not involved in the peer review process for this manuscript. The authors declare no other competing interests.

Author details

[1] A.I. Virtanen Institute for Molecular Sciences, University of Eastern Finland, Kuopio, Finland. [2] Institute of Biomedicine, University of Eastern Finland, Kuopio, Finland. [3] School of Pharmacy, Faculty of Health Sciences, University of Eastern Finland, Kuopio, Finland.

Received: 3 February 2025 Accepted: 8 April 2025
Published: 23 April 2025

References

1. Mason RT, Peterfreund RA, Sawchenko PE, Corrigan AZ, Rivier JE, Vale WW (1984) Release of the predicted calcitonin gene-related peptide from cultured rat trigeminal ganglion cells. Nature 308:653–655. https://doi.org/10.1038/308653a0
2. Ebersberger A, Averbeck B, Messlinger K, Reeh PW (1999) Release of substance P, calcitonin gene-related peptide and prostaglandin E2 from rat dura mater encephali following electrical and chemical stimulation in vitro. Neuroscience 89:901–907. https://doi.org/10.1016/S0306-4522(98)00366-2
3. Asghar MS, Hansen AE, Kapijimpanga T, Van Der Geest RJ, Van Der Koning P, Larsson HBW, Olesen J, Ashina M (2010) Dilation by CGRP of middle meningeal artery and reversal by sumatriptan in normal volunteers. Neurology 75:1520–1526. https://doi.org/10.1212/WNL.0b013e3181f9626a
4. Miller S, Liu H, Warfvinge K, Shi L, Dovlatyan M, Xu C, Edvinsson L (2016) Immunohistochemical localization of the calcitonin gene-related peptide binding site in the primate trigeminovascular system using functional antagonist antibodies. Neuroscience 328:165–183. https://doi.org/10.1016/j.neuroscience.2016.04.046
5. Levy D (2009) Migraine pain, meningeal inflammation, and mast cells. Curr Pain Headache Rep 13:237–240. https://doi.org/10.1007/s11916-009-0040-y
6. Strassman AM, Raymond SA, Burstein R (1996) Sensitization of meningeal sensory neurons and the origin of headaches. Nature 384:560–564. https://doi.org/10.1038/384560a0
7. Mungoven TJ, Meylakh N, Macefield VG, Macey PM, Henderson LA (2022) Alterations in brain structure associated with trigeminal nerve anatomy in episodic migraine. Front Pain Res 3:951581. https://doi.org/10.3389/fpain.2022.951581
8. Bolay H, Vuralli D, Goadsby PJ (2019) Aura and Head pain: relationship and gaps in the translational models. J Headache Pain 20:94. https://doi.org/10.1186/s10194-019-1042-8
9. Tottene A, Conti R, Fabbro A, Vecchia D, Shapovalova M, Santello M, Van Den Maagdenberg AMJM, Ferrari MD, Pietrobon D (2009) Enhanced Excitatory Transmission at Cortical Synapses as the Basis for Facilitated Spreading Depression in CaV2.1 Knockin Migraine Mice. Neuron 61:762–773. https://doi.org/10.1016/j.neuron.2009.01.027
10. Van Den Maagdenberg AMJM, Pietrobon D, Pizzorusso T, Kaja S, Broos LAM, Cesetti T, Van De Ven RCG, Tottene A, Van Der Kaa J, Plomp JJ, Frants RR, Ferrari MD (2004) A Cacna1a Knockin Migraine Mouse Model with Increased Susceptibility to Cortical Spreading Depression. Neuron 41:701–710. https://doi.org/10.1016/S0896-6273(04)00085-6
11. Schain AJ, Melo-Carrillo A, Stratton J, Strassman AM, Burstein R (2019) CSD-Induced Arterial Dilatation and Plasma Protein Extravasation Are Unaffected by Fremanezumab: Implications for CGRP's Role in Migraine with Aura. J Neurosci 39:6001–6011. https://doi.org/10.1523/JNEUROSCI.0232-19.2019
12. Wang Y, Tye AE, Zhao J, Ma D, Raddant AC, Bu F, Spector BL, Winslow NK, Wang M, Russo AF (2019) Induction of calcitonin gene-related peptide expression in rats by cortical spreading depression. Cephalalgia 39:333–341. https://doi.org/10.1177/0333102416678388
13. Kaag Rasmussen M, Møllgård K, Bork PAR, Weikop P, Esmail T, Drici L, Wewer Albrechtsen NJ, Carlsen JF, Huynh NPT, Ghitani N, Mann M, Goldman SA, Mori Y, Chesler AT, Nedergaard M (2024) Trigeminal ganglion neurons are directly activated by influx of CSF solutes in a migraine model. Science 385:80–86. https://doi.org/10.1126/science.adl0544
14. Della Pietra A, Savinainen J, Giniatullin R (2022) Inhibiting Endocannabinoid Hydrolysis as Emerging Analgesic Strategy Targeting a Spectrum of Ion Channels Implicated in Migraine Pain. Int J Mol Sci 23:4407. https://doi.org/10.3390/ijms23084407
15. Leimuranta P, Khiroug L, Giniatullin R (2018) Emerging Role of (Endo)Cannabinoids in Migraine. Front Pharmacol 9:420. https://doi.org/10.3389/fphar.2018.00420
16. Chandwani B, Bradley BA, Pace A, Buse DC, Singh R, Kuruvilla D (2023) The Exploration of Cannabis and Cannabinoid Therapies for Migraine. Curr Pain Headache Rep 27:339–350. https://doi.org/10.1007/s11916-023-01144-z
17. Zorrilla E, Della Pietra A, Russo AF (2024) Interplay between cannabinoids and the neuroimmune system in migraine. J Headache Pain 25:178. https://doi.org/10.1186/s10194-024-01883-3
18. Rodríguez-Muñoz M, Sánchez-Blázquez P, Merlos M, Garzón-Niño J (2016) Endocannabinoid control of glutamate NMDA receptors: the therapeutic potential and consequences of dysfunction. Oncotarget 7:55840–55862. https://doi.org/10.18632/oncotarget.10095
19. Eroli F, Loonen ICM, Van Den Maagdenberg AMJM, Tolner EA, Nistri A (2018) Differential neuromodulatory role of endocannabinoids in the rodent trigeminal sensory ganglion and cerebral cortex relevant to pain processing. Neuropharmacology 131:39–50. https://doi.org/10.1016/j.neuropharm.2017.12.013
20. Kazemi H, Rahgozar M, Speckmann E-J, Gorji A (2012) Effect of cannabinoid receptor activation on spreading depression. Iran J Basic Med Sci 15:926–936
21. Ibrahim MM, Rude ML, Stagg NJ, Mata HP, Lai J, Vanderah TW, Porreca F, Buckley NE, Makriyannis A, Malan PT (2006) CB2 cannabinoid receptor mediation of antinociception. Pain 122:36–42. https://doi.org/10.1016/j.pain.2005.12.018
22. Quartilho A, Mata HP, Ibrahim MM, Vanderah TW, Porreca F, Makriyannis A, Malan TP (2003) Inhibition of Inflammatory Hyperalgesia by Activation of Peripheral CB2Cannabinoid Receptors. Anesthesiology 99:955–960. https://doi.org/10.1097/00000542-200310000-00031
23. Sun J, Zhou Y-Q, Chen S-P, Wang X, Xu B-Y, Li D-Y, Tian Y-K, Ye D-W (2019) The endocannabinoid system: Novel targets for treating cancer induced bone pain. Biomed Pharmacother 120:109504. https://doi.org/10.1016/j.biopha.2019.109504
24. Akerman S, Kaube H, Goadsby PJ (2004) Anandamide Is Able to Inhibit Trigeminal Neurons Using an in Vivo Model of Trigeminovascular-Mediated Nociception. J Pharmacol Exp Ther 309:56–63. https://doi.org/10.1124/jpet.103.059808
25. Greco R, Demartini C, Zanaboni AM, Piomelli D, Tassorelli C (2018) Endocannabinoid System and Migraine Pain: An Update. Front Neurosci 12:172. https://doi.org/10.3389/fnins.2018.00172
26. Pracucci E, Pillai V, Lamers D, Parra R, Landi S (2021) Neuroinflammation: A Signature or a Cause of Epilepsy? Int J Mol Sci 22:6981. https://doi.org/10.3390/ijms22136981
27. Cravatt BF, Demarest K, Patricelli MP, Bracey MH, Giang DK, Martin BR, Lichtman AH (2001) Supersensitivity to anandamide and enhanced endogenous cannabinoid signaling in mice lacking fatty acid amide hydrolase. Proc Natl Acad Sci 98:9371–9376. https://doi.org/10.1073/pnas.161191698
28. Dinh TP, Carpenter D, Leslie FM, Freund TF, Katona I, Sensi SL, Kathuria S, Piomelli D (2002) Brain monoglyceride lipase participating in endocannabinoid inactivation. Proc Natl Acad Sci 99:10819–10824. https://doi.org/10.1073/pnas.152334899
29. Blankman JL, Simon GM, Cravatt BF (2007) A Comprehensive Profile of Brain Enzymes that Hydrolyze the Endocannabinoid 2-Arachidonoylglycerol. Chem Biol 14:1347–1356. https://doi.org/10.1016/j.chembiol.2007.11.006
30. Van Egmond N, Straub VM, Van Der Stelt M (2021) Targeting Endocannabinoid Signaling: FAAH and MAG Lipase Inhibitors. Annu Rev Pharmacol Toxicol 61:441–463. https://doi.org/10.1146/annurev-pharmtox-030220-112741
31. Della Pietra A, Giniatullin R, Savinainen JR (2021) Distinct Activity of Endocannabinoid-Hydrolyzing Enzymes MAGL and FAAH in Key Regions of Peripheral and Central Nervous System Implicated in Migraine. Int J Mol Sci 22:1204. https://doi.org/10.3390/ijms22031204
32. Della Pietra A, Krivoshein G, Ivanov K, Giniatullina R, Jyrkkänen H-K, Leinonen V, Lehtonen M, Van Den Maagdenberg AMJM, Savinainen J, Giniatullin R (2023) Potent dual MAGL/FAAH inhibitor AKU-005 engages endocannabinoids to diminish meningeal nociception implicated in migraine pain. J Headache Pain 24:38. https://doi.org/10.1186/s10194-023-01568-3
33. Marrs WR, Blankman JL, Horne EA, Thomazeau A, Lin YH, Coy J, Bodor AL, Muccioli GG, Hu SS-J, Woodruff G, Fung S, Lafourcade M, Alexander JP, Long JZ, Li W, Xu C, Möller T, Mackie K, Manzoni OJ, Cravatt BF, Stella N

(2010) The serine hydrolase ABHD6 controls the accumulation and efficacy of 2-AG at cannabinoid receptors. Nat Neurosci 13:951–957. https://doi.org/10.1038/nn.2601
34. Aaltonen N, Savinainen JR, Ribas CR, Rönkkö J, Kuusisto A, Korhonen J, Navia-Paldanius D, Häyrinen J, Takabe P, Käsnänen H, Pantsar T, Laitinen T, Lehtonen M, Pasonen-Seppänen S, Poso A, Nevalainen T, Laitinen JT (2013) Piperazine and Piperidine Triazole Ureas as Ultrapotent and Highly Selective Inhibitors of Monoacylglycerol Lipase. Chem Biol 20:379–390. https://doi.org/10.1016/j.chembiol.2013.01.012
35. Greco R, Demartini C, Francavilla M, Zanaboni AM, Facchetti S, Palmisani M, Franco V, Tassorelli C (2024) Effects of the Dual FAAH/MAGL Inhibitor AKU-005 on Trigeminal Hyperalgesia in Male Rats. Cells 13:830. https://doi.org/10.3390/cells13100830
36. Tang YT, Mendez JM, Theriot JJ, Sawant PM, López-Valdés HE, Ju YS, Brennan KC (2014) Minimum conditions for the induction of cortical spreading depression in brain slices. J Neurophysiol 112:2572–2579. https://doi.org/10.1152/jn.00205.2014
37. Vitale M, Tottene A, Zarin Zadeh M, Brennan K, Pietrobon D (2023) Mechanisms of initiation of cortical spreading depression. J Headache Pain 24:105. https://doi.org/10.1186/s10194-023-01643-9
38. Navia-Paldanius D, Patel JZ, López Navarro M, Jakupović H, Goffart S, Pasonen-Seppänen S, Nevalainen TJ, Jääskeläinen T, Laitinen T, Laitinen JT, Savinainen JR (2016) Chemoproteomic, biochemical and pharmacological approaches in the discovery of inhibitors targeting human α/β-hydrolase domain containing 11 (ABHD11). Eur J Pharm Sci 93:253–263. https://doi.org/10.1016/j.ejps.2016.08.031
39. Navia-Paldanius D, Savinainen JR, Laitinen JT (2012) Biochemical and pharmacological characterization of human α/β-hydrolase domain containing 6 (ABHD6) and 12 (ABHD12). J Lipid Res 53:2413–2424. https://doi.org/10.1194/jlr.M030411
40. Lehtonen M, Storvik M, Malinen H, Hyytiä P, Lakso M, Auriola S, Wong G, Callaway JC (2011) Determination of endocannabinoids in nematodes and human brain tissue by liquid chromatography electrospray ionization tandem mass spectrometry. J Chromatogr B 879:677–694. https://doi.org/10.1016/j.jchromb.2011.02.004
41. Savinainen JR, Yoshino M, Minkkilä A, Nevalainen T, Laitinen JT (2010) Characterization of binding properties of monoglyceride lipase inhibitors by a versatile fluorescence-based technique. Anal Biochem 399:132–134. https://doi.org/10.1016/j.ab.2009.12.009
42. Somjen GG (2001) Mechanisms of Spreading Depression and Hypoxic Spreading Depression-Like Depolarization. Physiol Rev 81:1065–1096. https://doi.org/10.1152/physrev.2001.81.3.1065
43. Liktor-Busa E, Levine AA, Palomino SM, Singh S, Wahl J, Vanderah TW, Stella N, Largent-Milnes TM (2023) ABHD6 and MAGL control 2-AG levels in the PAG and allodynia in a CSD-induced periorbital model of headache. Front Pain Res 4:1171188. https://doi.org/10.3389/fpain.2023.1171188
44. Walter L, Franklin A, Witting A, Wade C, Xie Y, Kunos G, Mackie K, Stella N (2003) Nonpsychotropic Cannabinoid Receptors Regulate Microglial Cell Migration. J Neurosci 23:1398–1405. https://doi.org/10.1523/JNEUROSCI.23-04-01398.2003
45. Pusic KM, Pusic AD, Kemme J, Kraig RP (2014) Spreading depression requires microglia and is decreased by their M2a polarization from environmental enrichment. Glia 62:1176–1194. https://doi.org/10.1002/glia.22672
46. Zhang Y, Gilliam A, Maitra R, Damaj MI, Tajuba JM, Seltzman HH, Thomas BF (2010) Synthesis and Biological Evaluation of Bivalent Ligands for the Cannabinoid 1 Receptor. J Med Chem 53:7048–7060. https://doi.org/10.1021/jm1006676
47. Borroto-Escuela DO, Romero-Fernandez W, Rivera A, Van Craenenbroeck K, Tarakanov AO, Agnati LF, Fuxe K (2013) On the G-Protein-Coupled Receptor Heteromers and Their Allosteric Receptor-Receptor Interactions in the Central Nervous System: Focus on Their Role in Pain Modulation. Evid Based Complement Alternat Med 2013:1–17. https://doi.org/10.1155/2013/563716
48. Fuxe K, Borroto-Escuela DO (2016) Heteroreceptor Complexes and their Allosteric Receptor-Receptor Interactions as a Novel Biological Principle for Integration of Communication in the CNS: Targets for Drug Development. Neuropsychopharmacology 41:380–382. https://doi.org/10.1038/npp.2015.244
49. Colín-González AL, Aguilera G, Santamaría A (2016) Cannabinoids: Glutamatergic Transmission and Kynurenines. In: Essa MM, Akbar M, Guillemin G (eds) The Benefits of Natural Products for Neurodegenerative Diseases. Springer International Publishing, Cham, pp 173–198
50. Shatillo A, Salo RA, Giniatullin R, Gröhn OH (2015) Involvement of NMDA receptor subtypes in cortical spreading depression in rats assessed by fMRI. Neuropharmacology 93:164–170. https://doi.org/10.1016/j.neuropharm.2015.01.028
51. Nagy-Grócz G, Zádor F, Dvorácskó S, Bohár Z, Benyhe S, Tömböly C, Párdutz Á, Vécsei L (2017) Interactions between the Kynurenine and the Endocannabinoid System with Special Emphasis on Migraine. Int J Mol Sci 18:1617. https://doi.org/10.3390/ijms18081617
52. Brennan KC, Romero-Reyes M, López Valdés HE, Arnold AP, Charles AC (2007) Reduced threshold for cortical spreading depression in female mice. Ann Neurol 61:603–606. https://doi.org/10.1002/ana.21138
53. Kudo C, Harriott AM, Moskowitz MA, Waeber C, Ayata C (2023) Estrogen modulation of cortical spreading depression. J Headache Pain 24:62. https://doi.org/10.1186/s10194-023-01598-x
54. Tozzi A, De Iure A, Di Filippo M, Costa C, Caproni S, Pisani A, Bonsi P, Picconi B, Cupini LM, Materazzi S, Geppetti P, Sarchielli P, Calabresi P (2012) Critical role of calcitonin gene-related peptide receptors in cortical spreading depression. Proc Natl Acad Sci 109:18985–18990. https://doi.org/10.1073/pnas.1215435109
55. Holton CM, Strother LC, Dripps I, Pradhan AA, Goadsby PJ, Holland PR (2020) Acid-sensing ion channel 3 blockade inhibits durovascular and nitric oxide-mediated trigeminal pain. Br J Pharmacol 177:2478–2486. https://doi.org/10.1111/bph.14990
56. Aaltonen N, Singha PK, Jakupović H, Wirth T, Samaranayake H, Pasonen-Seppänen S, Rilla K, Varjosalo M, Edgington-Mitchell LE, Kasperkiewicz P, Drag M, Kälvälä S, Moisio E, Savinainen JR, Laitinen JT (2020) High-Resolution Confocal Fluorescence Imaging of Serine Hydrolase Activity in Cryosections – Application to Glioma Brain Unveils Activity Hotspots Originating from Tumor-Associated Neutrophils. Biol Proced Online 22:6. https://doi.org/10.1186/s12575-020-00118-4

Publisher's Note